

Direct Analysis of Spectra of the Unusual Type Ib Supernova 2005bf

Jerod Parrent¹, David Branch¹, M. A. Troxel¹, D. Casebeer¹, David J. Jeffery¹,
W. Ketchum¹, E. Baron¹, F. J. D. Serduke², and Alexei V. Filippenko²

ABSTRACT

Synthetic spectra generated with the parameterized supernova synthetic-spectrum code SYNOW are compared to spectra of the unusual Type Ib supernova 2005bf. We confirm the discovery by Folatelli et al. (2006) that very early spectra (~ 30 days before maximum light) contain both photospheric-velocity (~ 8000 km s⁻¹) features of He I, Ca II, and Fe II, and detached high-velocity ($\sim 14,000$ km s⁻¹) features of H α , Ca II, and Fe II. An early spectrum of SN 2005bf is an almost perfect match to a near-maximum-light spectrum of the Type Ib SN 1999ex. Although these two spectra were at very different times with respect to maximum light (20 days before maximum for SN 2005bf and five days after for SN 1999ex), they were for similar times after explosion — about 20 days for SN 2005bf and 24 days for SN 1999ex. The almost perfect match clinches the previously suggested identification of H α in SN 1999ex and supports the proposition that many if not all Type Ib supernovae eject a small amount of hydrogen. The earliest available spectrum of SN 2005bf resembles a near-maximum-light spectrum of the Type Ic SN 1994I. These two spectra also were at different times with respect to maximum light (32 days before maximum for SN 2005bf and four days before for SN 1994I) but at similar times after explosion — about eight days for SN 2005bf and 10 days for SN 1994I. The resemblance motivates us to consider a reinterpretation of the spectra of Type Ic supernovae, involving coexisting photospheric-velocity and high-velocity features. The implications of our results for the geometry of the SN 2005bf ejecta, which has been suggested to be grossly asymmetric, are briefly discussed.

Subject headings: supernovae: general — supernovae: individual (SN 2005bf, SN 1999ex, SN 1994I)

¹Homer L. Dodge Department of Physics and Astronomy, University of Oklahoma, Norman, OK 73019; e-mail: parrent@nhn.ou.edu, branch@nhn.ou.edu

²Department of Astronomy, University of California, Berkeley, CA 94720-3411

1. INTRODUCTION

Among the hydrogen-deficient Type I supernovae, the Type Ib (SN Ib) subclass is defined by the absence of strong Si II and the presence of He I lines in the optical spectra. Type Ic supernovae (SNe Ic) are broadly similar to SNe Ib, but lack conspicuous He I lines. SNe Ib and SNe Ic are generally thought to be core-collapse supernovae whose progenitor stars lost most, or all, of their hydrogen and helium envelopes, respectively. [See Filippenko (1997) for a review of supernova spectral types.]

Supernova 2005bf was an exceptionally interesting Type Ib event (Anupama et al. 2005; Tominaga et al. 2005; Folatelli et al. 2006; hereafter A05, T05, and F06, respectively). The bolometric light curve reached an initial maximum about 15 days after explosion but also a brighter second maximum (which hereafter we refer to as the maximum, without qualification) about 40 days after explosion. Such a double-peaked light curve and such a long rise time to maximum light had not been observed previously. Both T05 and F06 invoked a double-peaked radial distribution of ^{56}Ni to account for the light curve, although in other respects the models they discussed were quite different.

T05 and F06 attributed an absorption feature in very early spectra to $\text{H}\alpha$, forming at the high velocity of about $14,000 \text{ km s}^{-1}$, and F06 provided support for the identification by recognizing the presence of Ca II and Fe II features at the same velocity. A weaker absorption at the same wavelength in near-maximum-light spectra was attributed by A05 to $\text{H}\alpha$ and/or Si II $\lambda 6355$, while T05 favored Si II and F06 only remarked that by maximum light the early feature attributed to $\text{H}\alpha$ had disappeared. In view of the unusual nature of SN 2005bf, and of our interest in the issue of whether SNe Ib and even SNe Ic eject some hydrogen during their explosions (Filippenko 1992; Branch et al. 2006, hereafter B06), we have carried out a direct analysis of selected spectra of SN 2005bf using a revised version (2.0) of the parameterized resonance-scattering supernova synthetic-spectrum code, SYNOW.

Spectra of SN 2005bf are displayed and discussed in §2 and our analysis of them is presented in §3. In §4, the significance of relationships between the spectra of SN 2005bf, the Type Ib SN 1999ex (Hamuy et al. 2002), and the Type Ic SN 1994I (Filippenko et al. 1995) is explored. The implications of our results are discussed in §5.

2. OBSERVED SPECTRA

Twelve spectra of SN 2005bf are shown in Figure 1. Following F06, epochs are with respect to the date of bolometric maximum light, 9 May 2005 (UT dates are used throughout this paper). Maximum in the B band occurred about 2.5 days earlier. The day -6 , -4 , and

–2 spectra are from A05. The previously unpublished day +5 spectrum was obtained with the 3-m Shane reflector at Lick Observatory using the Kast spectrograph (Miller & Stone 1993); observations and reductions were similar to those of the day +2 spectrum, which was presented and described in F06. The other eight spectra also are from F06. Mild smoothing has been applied to some of the spectra. Because in this paper we are interested only in the spectral features, not in the shape of the underlying continuum, all observed and synthetic spectra are “flattened” by means of the local normalization prescription of Jeffery et al. (2007).

From left to right, the dashed lines in Figure 1 correspond to He I $\lambda 5876$ blueshifted by 7000 km s^{-1} , H α $\lambda 6563$ blueshifted by $15,000 \text{ km s}^{-1}$, and He I $\lambda 6678$ and $\lambda 7065$ blueshifted by 7000 km s^{-1} . He I absorptions blueshifted by about 7000 km s^{-1} are clearly present at all epochs. [From careful measurements of the wavelength of the absorption minimum attributed to He I $\lambda 5876$, T05 noticed that the blueshift increased slightly with time. This may have been due to the increasing strength of the feature; all else being equal, stronger features have higher blueshifts (Jeffery & Branch 1990).] The deep absorption attributed to high-velocity H α at early times becomes weaker between day –20 and day –6, but a feature persists at close to the same wavelength as late as day +5.

3. ANALYSIS

For the analysis presented in this paper we have used a revised version (2.0) of SYNOW¹ that is described by Branch et al. (2007). New features employed here are (1) when using power-law line optical depth profiles, different power-law indices can be adopted for different ions; (2) a Gaussian line optical depth profile is now available, so that when detaching an ion from the photosphere it is not necessary to introduce a discontinuity in the line optical depth profile; and (3) the output spectra can be flattened as in Jeffery et al. (2007). For this paper the excitation temperature (T_{exc}) has been fixed at a nominal value of 7000 K. For ions that are not detached from the photosphere a power-law line optical depth distribution $\tau(v) = \tau_p(v/v_{phot})^{-n}$ is used, where v_{phot} and τ_p are the velocity and the line optical depth at the photosphere. We use $n = 8$ as the default value of the power-law index, but other values are occasionally adopted to improve the fits. For ions that are detached from the photosphere a Gaussian line optical depth distribution $\tau(v) = \tau_g \exp^{-((v-v_g)/\sigma_g)^2}$ is used, i.e., the maximum line optical depth τ_g occurs at velocity v_g . We refer to ions that are undetached or only mildly detached as photospheric velocity (PV) ions and those that are detached at

¹Version 2.0 will soon be available at <http://nhn.ou.edu/~parrent/download.html>.

high velocity relative to the photosphere as HV ions.

In this section we will cover some of the same ground as F06. (The necessity of doing so was reinforced for us when we learned that the expert referee of this paper was not convinced of the HV Fe II identification by F06 or by the first version of this paper.) In this paper we provide all of the synthetic-spectrum fitting parameters (unlike F06), and thanks to mild smoothing of the observed spectra and to the scale on which the fits are published, our fits can be examined more closely than those of F06.

3.1. Early Spectra

Figure 2 shows a close-up view of the multiplet-42 region of Fe II for the four early spectra. The long dashed lines correspond to $\lambda 4924$, $\lambda 5018$, and $\lambda 5169$, blueshifted by $13,000 \text{ km s}^{-1}$. Absorptions consistent with these transitions are clearly present in the day -32 , -27 , and -24 spectra. The short solid lines correspond to the same transitions blueshifted by 7000 km s^{-1} . The four early spectra have been compared with SYNOW spectra. Our interpretation of them is in good agreement with that of F06, although our results differ in detail because, for example, the version of SYNOW available to F06 did not have the Gaussian option.

In Figure 3 the day -32 spectrum is compared with a synthetic spectrum that has $v_{\text{phot}} = 8000 \text{ km s}^{-1}$ and includes lines of PV He I, O I, and Fe II, as well as HV H I, Ca II, and Fe II. (The parameters of all synthetic spectra of this paper are mentioned in the text and/or listed in Table 1.) In the synthetic spectrum PV He I is responsible for three features and PV O I $\lambda 7773$ is responsible for one. The main (but not only) role of PV Fe II is to produce the dip in the synthetic spectrum near 5040 \AA . The influence of the HV ions is greater than that of the PV ions. The HV Ca II infrared triplet produces the deep absorption near 8110 \AA , and HV Fe II produces absorptions near 4930 , 4790 , 4710 , and 4560 \AA , and HV H α produces the deep absorption near 6210 \AA . The v_g values for HV Ca II and H I are $17,000 \text{ km s}^{-1}$ while that of Fe II is $15,000 \text{ km s}^{-1}$. We consider the HV Ca II, H α , and Fe II identifications to be definite. Figure 4 is like Figure 3 except that HV Fe II has been removed. We know of no way to restore the good fit of Figure 3 without using HV Fe II.

In Figure 5 the day -27 spectrum is compared with a synthetic spectrum that is much like that of Figure 3 for day -32 , but in Figure 5 $v_{\text{phot}} = 7000 \text{ km s}^{-1}$ and PV Ca II is introduced. (The difference between $v_{\text{phot}} = 8000 \text{ km s}^{-1}$ for day -32 and $v_{\text{phot}} = 7000 \text{ km s}^{-1}$ for day -27 is within our fitting uncertainties.) The HV and PV Ca II parameters are chosen to produce a reasonable fit to the P-Cygni profile extending from about 8000 \AA

to 8800 Å. The main changes between the synthetic spectra for day –32 and day –27 are that $\tau_p(\text{He I})$ has increased by a factor of 1.5, $\tau_g(\text{HV Ca II})$ has decreased by a factor of 6.25, and PV Ca II has been introduced with $\tau_p = 4$. T05 used a different synthetic-spectrum code, the Mazzali-Lucy Monte Carlo code (Mazzali 2000), to fit a day –26 spectrum. They attributed the 6210 Å absorption to a blend of HV H α and PV Si II, and they did not explicitly² introduce HV Ca II and Fe II features. (Their day –26 spectrum did not extend far enough to the red to show the HV Ca II absorption at 8000 Å.)

Between days –27 and –24 there are no major changes in our synthetic-spectrum parameters (see Table 1). In Figure 6 the day –20 spectrum is compared with a synthetic spectrum that has $v_{\text{phot}} = 8000 \text{ km s}^{-1}$. The major changes compared to day –27 are that for day –20 HV Fe II is not used at all, $\tau_p(\text{PV Ca II})$ has increased by a factor of 12.5, and $\tau_p(\text{PV Fe II})$ has increased by a factor of 10.

Significant spectral evolution occurred between days –32 and –20, especially between days –24 and –20. The day –32 spectrum is strongly influenced by HV features, but PV features also are present. By day –20, the spectrum is mainly PV, the only HV feature being H α . From day –32 to day –20, $\tau_p(\text{He I})$ increased by a factor of two, suggestive of increasing nonthermal excitation (T05), while the fitting parameters for H α varied only mildly.

3.2. Maximum Light

The five spectra of Figure 1 from day –6 to day +5 are rather similar, so we consider only day +2 here. In Figure 7 the day +2 spectrum is compared with a synthetic spectrum that has $v_{\text{phot}} = 7000 \text{ km s}^{-1}$ and includes lines of PV He I, O I, Ca II, and Fe II, as well as HV H I. A05 noted that in the day –6 spectrum the Fe II absorptions were more blueshifted than the He I absorptions. We find the same for the day +2 spectrum: in the synthetic spectrum of Figure 7 Fe II lines are mildly detached,³ at 8000 km s^{–1}, while the He I lines are not.

T05 found that in a day –5 spectrum Si II was satisfactory for the absorption that we attribute to H α . Figure 8, which is like Figure 7 except that HV H I has been replaced

²In principle, since T05 input density and abundance, not line optical depth, their synthetic spectra could have contained HV Ca II and Fe II features.

³Strictly speaking, an ion is not detached if its line optical depth reaches a maximum value above the photosphere but is not negligible at the photosphere, as is the case here. Nevertheless, for brevity we refer to such cases as detached.

by PV Si II ($\tau_p=1$, $n=8$), shows that for us the Si II absorption has its usual problem in SN Ib/c spectra: it is too blue to account for the observed absorption on its own. The synthetic spectrum of T05 has $v_{\text{phot}}=4600 \text{ km s}^{-1}$, compared to our value of 7000 km s^{-1} , and from their Figure 4 it appears that many of the synthetic absorptions are insufficiently blueshifted. This may account for their finding that Si II is satisfactory.

3.3. Postmaximum

The latest three spectra of Figure 1 are similar, so we consider only day +21. In Figure 9 the day +21 spectrum is compared with a synthetic spectrum that has $v_{\text{phot}}=5000 \text{ km s}^{-1}$ and includes the same lines as in Figure 7 except that HV H I is not used — the synthetic spectrum is entirely PV. The observed absorptions near 5460 and 5590 Å could be fitted reasonably well with PV Sc II, but then Sc II $\lambda 4247$ would produce a deep unwanted absorption near 4100 Å. Part of the observed depression extending from 6290 to 6480 Å could be fit by introducing PV H α but the identification would not be convincing.

4. RELATIONSHIP TO SPECTRA OF SN 1999ex AND SN 1994I

F06 noted that the day -20 spectrum of SN 2005bf and a day $+5$ spectrum of the Type Ib SN 1999ex (Hamuy et al. 2002) were similar, in spite of the very different epochs with respect to maximum light. In Figure 10 the same two spectra are compared directly in a plot of linear flux and with both spectra flattened (F06 presented a log-flux plot of unflattened spectra). Figure 10 shows that the two spectra are almost identical! They are so similar that it is not plausible that two different interpretations apply. Only minor tweaking of the synthetic spectrum for day -20 of SN 2005bf (Figure 6), such as increasing the optical depth of HV Ca II, would produce an equally good synthetic spectrum for day $+5$ of SN 1999ex. As discussed above, the day -20 spectrum of SN 2005bf is dominated by PV features but also includes HV H α . The spectrum of SN 1999ex was interpreted in a similar way by B06, but the HV H α identification was perhaps not entirely convincing. Figure 10 clinches the HV H α identification in SN 1999ex.

To account for the fact that based on very early spectra, SN 2005bf was initially classified as a Type Ic (Morell et al. 2005; Modjaz, Kirshner, & Challis 2005), F06 also noted that to some extent the day -32 spectrum of SN 2005bf resembled a day -5 spectrum of the Type Ic SN 1994I (Filippenko et al. 1995). This leads us to ask whether the day -32 spectrum of SN 2005bf has something to teach us about how to interpret the near-maximum spectra of

SN 1994I. Figure 11 is like Figure 10, but for the day -32 spectrum of SN 2005bf and a day -4 spectrum of SN 1994I. The resemblance in Figure 11 is not as striking as in Figure 10, but it is sufficient to suggest that previous interpretations of the SN 1994I spectrum should be reconsidered. Millard et al. (1999), using the SYNOW code to interpret the day -4 spectrum of SN 1994I, did not consider the possibility that the spectrum was a composite HV and PV spectrum; therefore in order to fit the Ca II IR triplet feature they had to use a high value of $v_{\text{phot}} = 17,500 \text{ km s}^{-1}$. This led to difficulties in accounting for some of the other features. Millard et al. attributed the feature produced by He I $\lambda 5876$ in SN 2005bf to Na I (with an imposed maximum velocity) in SN 1994I, and the feature produced by HV $H\alpha$ in SN 2005bf as a blend of Si II (with an imposed maximum velocity) and (detached) C II in SN 1994I.

Here we briefly consider a reinterpretation of the day -4 spectrum of SN 1994I. Using the same ions as for the day -32 spectrum of SN 2005bf, we varied the SYNOW input parameters and obtained the fit shown in Figure 12. The synthetic spectrum has $v_{\text{phot}} = 12,000 \text{ km s}^{-1}$ (compared to 8000 km s^{-1} for SN 2005bf) and the values of v_g for HV H I, HV Ca II, and HV Fe II are $23,000$, $19,000$, and $18,000 \text{ km s}^{-1}$, respectively (compared to $17,000$, $17,000$, and $15,000 \text{ km s}^{-1}$ for SN 2005bf). The fit is encouraging (although to fit the Ca II infrared triplet we have had to make Ca II H&K too strong) and seems at least as plausible as that of Millard et al. (1999), as well as that of Sauer & Mazzali (2006) who also attributed features in SN 1994I to Na I and to a blend of Si II and C II (and Ne I). A more thorough reconsideration of the early spectra of SNe Ic is deferred to a separate paper.

B06 discussed the possible presence of HV $H\alpha$ and PV He I in spectra of SN 1994I, as well as the possible presence of PV $H\alpha$ as would be required by the tentative identification (Filippenko 1988, 1992) of centrally peaked $H\alpha$ emission in SN 1994I and other SNe Ic. (Centrally peaked emission cannot be produced by highly detached hydrogen.) Figure 13 is like Figure 12 but with PV $H\alpha$ included (with $\tau_p = 0.6$, $n = 8$). PV $H\alpha$ certainly does no harm; in fact, the fit is somewhat improved. It may be that PV $H\alpha$ actually is in net emission in SN 1994I, as it is in SNe II, rather than a resonance-scattering profile as given by SYNOW; net emission in the synthetic spectrum would improve the fit near 6563 \AA . The presence of PV $H\alpha$ in SNe Ic remains a possibility.

5. DISCUSSION

Our interpretation of the very early spectra, including the identification of HV $H\alpha$, is in good agreement with that of F06. In addition, we favor the $H\alpha$ identification as late as day $+2$, and perhaps even day $+5$. Wang & Baade (2005) reported that an unpublished

spectrum obtained on day -9 (presumably a very high signal-to-noise spectrum, because spectropolarimetry was obtained) appeared to contain $H\beta$ and $H\gamma$ absorptions. This increases our confidence in the $H\alpha$ identification⁴ at day $+2$.

F06 discussed models for SN 2005bf. Although the numerical results they presented were based on spherical symmetry, they envisaged a grossly asymmetric explosion having many features in common with the supernovae that are associated with gamma-ray bursts, for which the most popular model is the collapsar model (Woosley & Bloom 2006, and references therein). In SN 2005bf, according to F06, a collapsar launched relativistic jets that drove a small fraction of the ejected matter into high-velocity ($v \gtrsim 14,000 \text{ km s}^{-1}$) bipolar flows that contained about $0.1 M_{\odot}$ per pole of ^{56}Ni , were optically thick at early times, and produced the first light-curve peak. When the bipolar ejecta became optically thin, the underlying low-velocity ejecta, primarily equatorial and containing most of the mass and ^{56}Ni , powered the main light-curve peak. It should be noted, though, that the presence of PV features in the early spectra shows that the bipolar flows were *not* optically thick at the time of the first peak. Another issue is the distribution of hydrogen with respect to velocity. The progenitor star contained a surface layer of hydrogen. If the bipolar flows are of sufficiently wide opening angle, it may be that a pole-on observer sees only HV hydrogen in absorption, not PV hydrogen. But an equator-on observer would see PV hydrogen in absorption. Equator-on is statistically more likely than pole-on, yet it is not clear that any SN Ib/c has been seen to have PV, but not HV, hydrogen. Thus the F06 interpretation of SN 2005bf requires that SN 2005bf-like events are quite uncommon; otherwise, SNe Ib/c with PV but not HV hydrogen in absorption should be found.

Like F06, T05 argued that the double-peaked light curve required a double-peaked radial distribution of ^{56}Ni , but T05 invoked jets that were not sufficiently energetic to reach the bottom of the helium layer, at $v \simeq 6000 \text{ km s}^{-1}$; these jets provided a small amount of ^{56}Ni at intermediate velocities ($3900 \lesssim v \lesssim 5400 \text{ km s}^{-1}$) to power the first peak.⁵ Based on several perceived similarities, T05 suggested that SN 2005bf may have been a Cas A-like event. The T05 model is not necessarily highly asymmetric,⁶ so all of the hydrogen could

⁴Soderberg et al. (2005) reported that at day 175 the nebular spectrum was dominated by strong, broad (FWHM $\sim 3400 \text{ km s}^{-1}$) $H\alpha$ emission, but this emission may have been circumstellar rather than from low-velocity ejecta.

⁵The referee asks us to mention that both F06 and T05 had to make the unphysical assumption that the gamma-ray opacity abruptly decreased in order to simulate the rapid decline of the light curve after the second peak.

⁶But in order to fit the rapid post-maximum decline of the light curve, both T05 and F06 had to assume a rapid drop in the gamma-ray opacity, which could be a consequence of strong asymmetry.

be ejected at high velocity, and the issue of seeing SNe Ib/c with PV but not HV hydrogen does not necessarily arise.

In view of the almost perfect resemblance of the day +5 spectrum of SN 1999ex and the day –20 spectrum of SN 2005bf (Fig. 8), we regard the identification of H α in SN 1999ex as definite. This supports the proposition that most SNe Ib eject some hydrogen (Deng et al. 2000; Branch et al. 2002; Elmhamdi et al. 2006). To our knowledge, there is no published, clear explanation why hydrogen should generally not be entirely removed from the progenitors of supernovae that develop conspicuous He I lines.

The resemblance of the day +5 spectrum of SN 1999ex and the day –20 spectrum of SN 2005bf means that at these epochs the conditions near the photosphere — composition, density structure, and temperature — were very similar. It is interesting to note (a) that for SN 2005bf day –20 corresponds to about day +5 with respect to the *initial* maximum, and (b) that these epochs correspond to similar times after explosion — 20 days for SN 2005bf and 24 days for SN 1999ex [assuming a rise time for SN 1999ex of 19 days (Richardson, Branch, & Baron 2006)]. But although the conditions at the photosphere were similar at these epochs, what was to follow — to be determined by what was still *beneath* the photosphere — would be very different.

Similarly, the times with respect to explosion for the day –4 spectrum of SN 1994I and the day –32 spectrum of SN 2005bf (Fig. 10) are not very different — about eight days for SN 2005bf and 10 days for SN 1994I [assuming a rise time for SN 1994I of 14 days (Richardson et al 2006)]. The similarities between these two spectra raise our suspicion that SN 1994I ejected hydrogen. If so, then most or all other ordinary SNe Ic also do (see B06), and they are not explosions of bare carbon-oxygen cores as they usually are modelled. If SN 1994I did *not* eject hydrogen, then the spectroscopic coincidences between SNe Ib that do eject hydrogen and SNe Ic that do not eject hydrogen are even more striking than they appeared to B06.

We are grateful to G. Anupama and G. Folatelli for providing spectra. We also thank the staffs at the Lick and Keck Observatories for this assistance. This work has been supported by NSF grants AST–0204771, AST–0506028, and AST–0607485, as well as by NASA LTSA grant NNG04GD36G.

REFERENCES

- Anupama, G. C., et al. 2005, *ApJ*, 631, L125 (A05)
- Branch, D., Jeffery, D. J., Young, T. R., & Baron, E. 2006, *PASP*, 118, 791 (B06)
- Branch, D., Parrent, J., Troxel, M. A., Casebeer, D., Jeffery, D. J., Baron, E., Ketchum, W., & Hall, N. in *The Multicoloured Landscape of Compact Objects and their Explosive Origins*, ed. L. Burderi, et al. (Melville, New York: AIP), in press
- Branch, D., et al. 2002, *ApJ*, 566, 1005
- Deng, J. S., Qiu, Y. L., Hu, J. Y., Hatano, K., & Branch, D. 2000, *ApJ*, 540, 452
- Elmhamdi, A., Danziger, I. J., Branch, D., Leibundgut, B., Baron, E. & Kirshner, R. P. 2006, *A&A*, 450, 305
- Filippenko, A. V. 1988, *AJ*, 96, 1941
- Filippenko, A. V. 1992, *ApJ*, 384, L37
- Filippenko, A. V. 1997, *ARAA*, 35, 309
- Filippenko, A. V., et al. 1995, *ApJ*, 450, L11
- Folatelli, G., et al. 2006, *ApJ*, 641, 1039 (F06)
- Hamuy, M., et al. 2002, *AJ*, 124, 417
- Jeffery, D. J., & Branch, D., 1990, in *Supernovae*, ed. J. C. Wheeler, T. Piran, & S. Weinberg (Singapore: World Scientific), 90
- Jeffery, D. J., Ketchum, W., Branch, D., Baron, E., Elmhamdi, A., & Danziger, I. J. 2007, *ApJS*, submitted; astro-ph/0607084
- Kurucz, R. L. 1993, CD-ROM 1, *Atomic Data for Opacity Calculations* (Cambridge: SAO)
- Mazzali, P. A. 2000, *A&A*, 363, 705
- Millard, J., et al. 1999, *ApJ*, 527, 746
- Miller, J. S., & Stone, R. P. S. 1993, *Lick Observatory Technical Report No. 66*
- Modjaz, M., Kirshner, R. P., & Challis, P. 2005, *IAU Circ.*, 8509
- Morrell, N., Hamuy, M., Folatelli, G., & Contreras, C. 2005, *IAU Circ.*, 8509
- Richardson, D., Branch, D., & Baron, E. 2006, *AJ*, 131, 2233
- Sauer, D. N., Mazzali, P. A., Deng, J., Valenti, S., Nomoto, K., & Filippenko, A. V. 2006, *MNRAS*, 369, 1939
- Soderberg, A. M., Berger, E., Ofek, E., & Leonard, D. C. 2005, *Astr. Tel.*, 646

Tominaga, N., et al. 2005, ApJ, 633, L97 (T05)

Wang, L., & Baade, D. 2005, IAU Circ., 8521

Woosley, S. E., & Bloom, J. S. 2006, ARAA, 44, 507

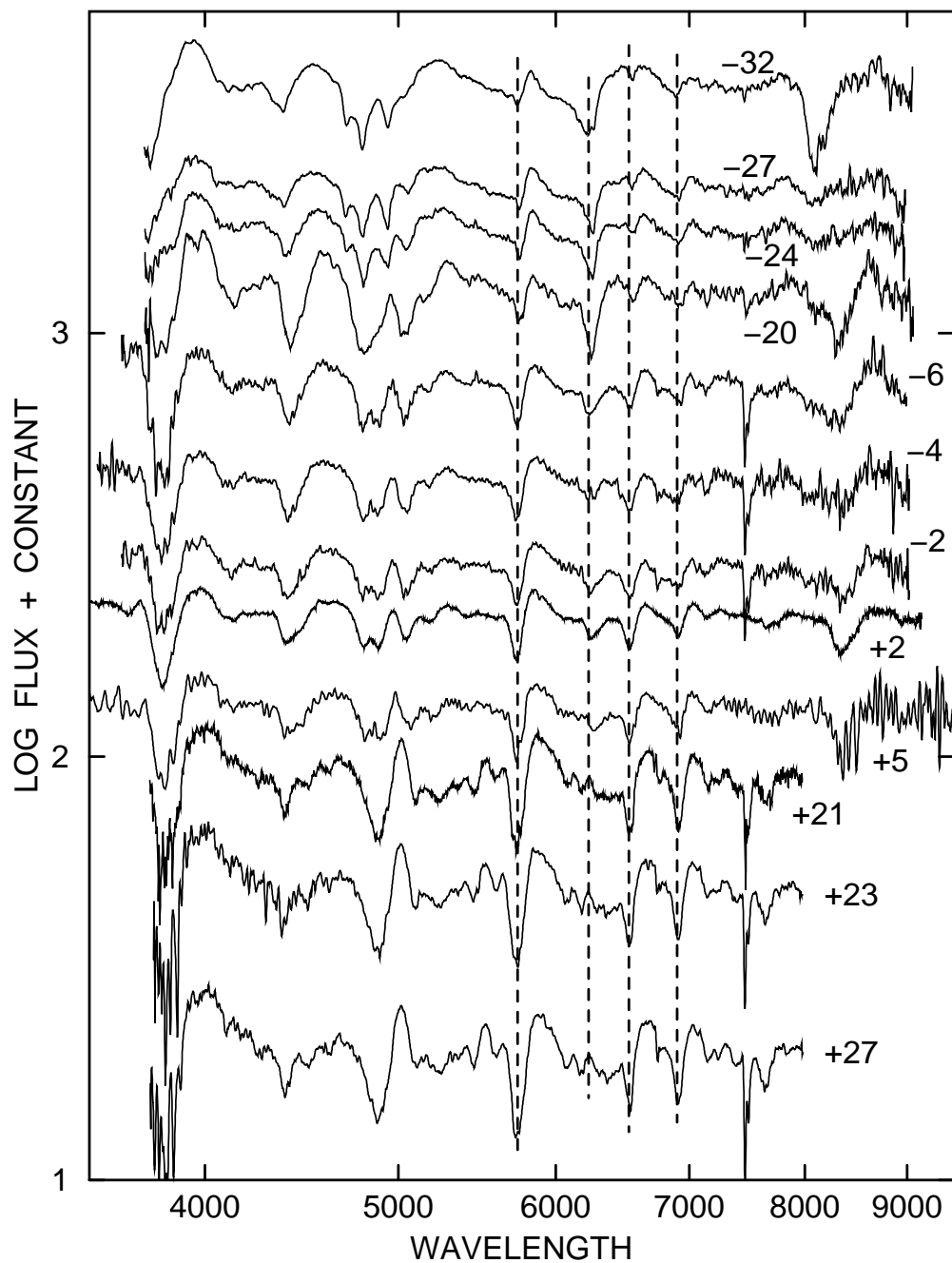


Fig. 1.— Spectra of SN 2005bf from A05 and F06, and a previously unpublished spectrum for day +5. The spectra have been corrected for $cz = 5496 \text{ km s}^{-1}$ (F06). The narrow absorption near 7460 \AA is telluric and vertical shifts are arbitrary. The spectra have been flattened by means of the local normalization prescription of Jeffery et al. (2007). The *dashed lines* are discussed in the text.

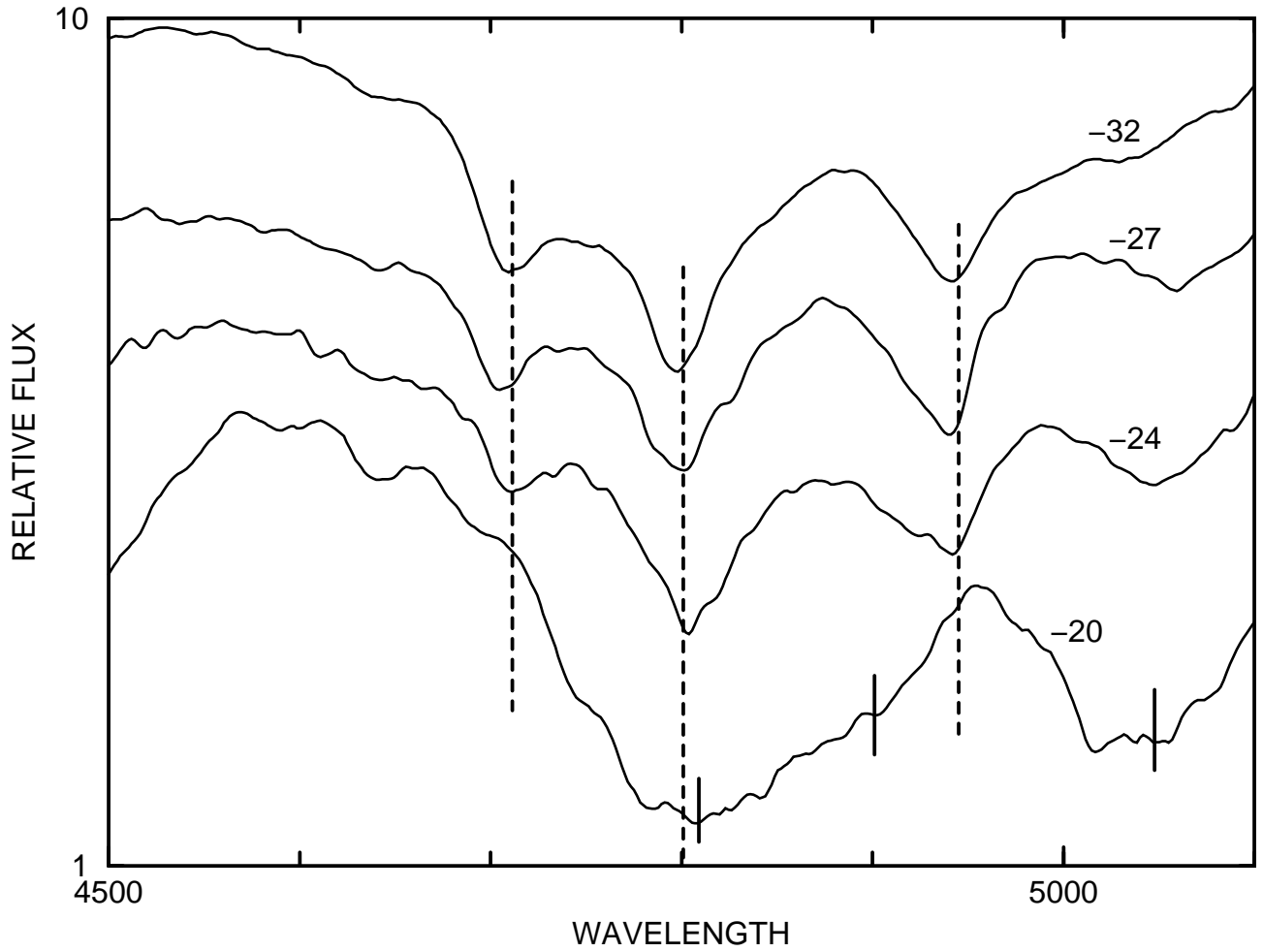


Fig. 2.— A close-up view of the multiplet-42 region of Fe II in the four earliest spectra of SN 2005bf, from F06. The long *dashed lines* correspond to Fe II $\lambda 4924$, $\lambda 5018$, and $\lambda 5169$ blueshifted by $13,000 \text{ km s}^{-1}$, and the short *solid lines* correspond to the same lines blueshifted by 7000 km s^{-1} .

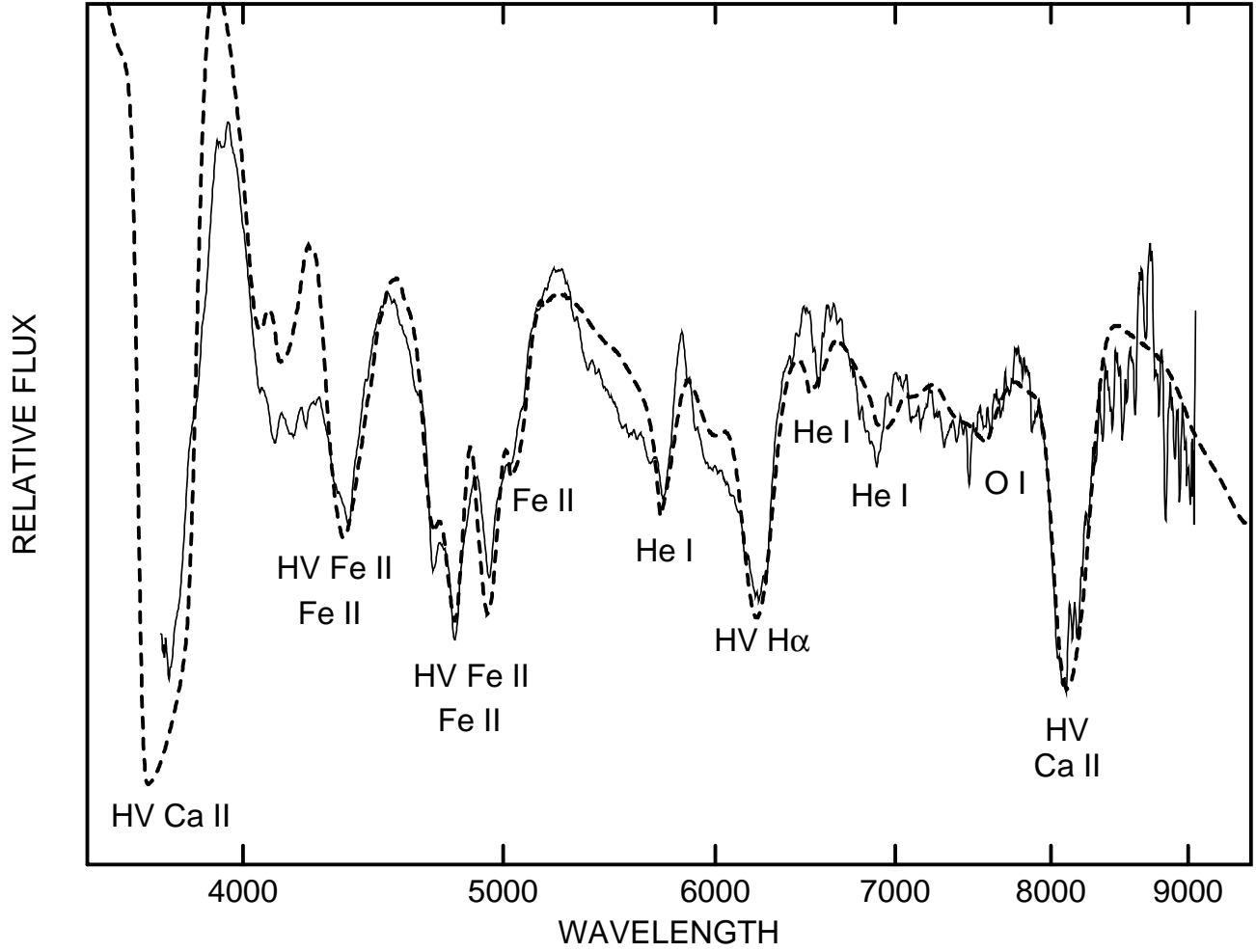


Fig. 3.— The day -32 spectrum of SN 2005bf (*solid line*) is compared with a synthetic spectrum (*dashed line*).

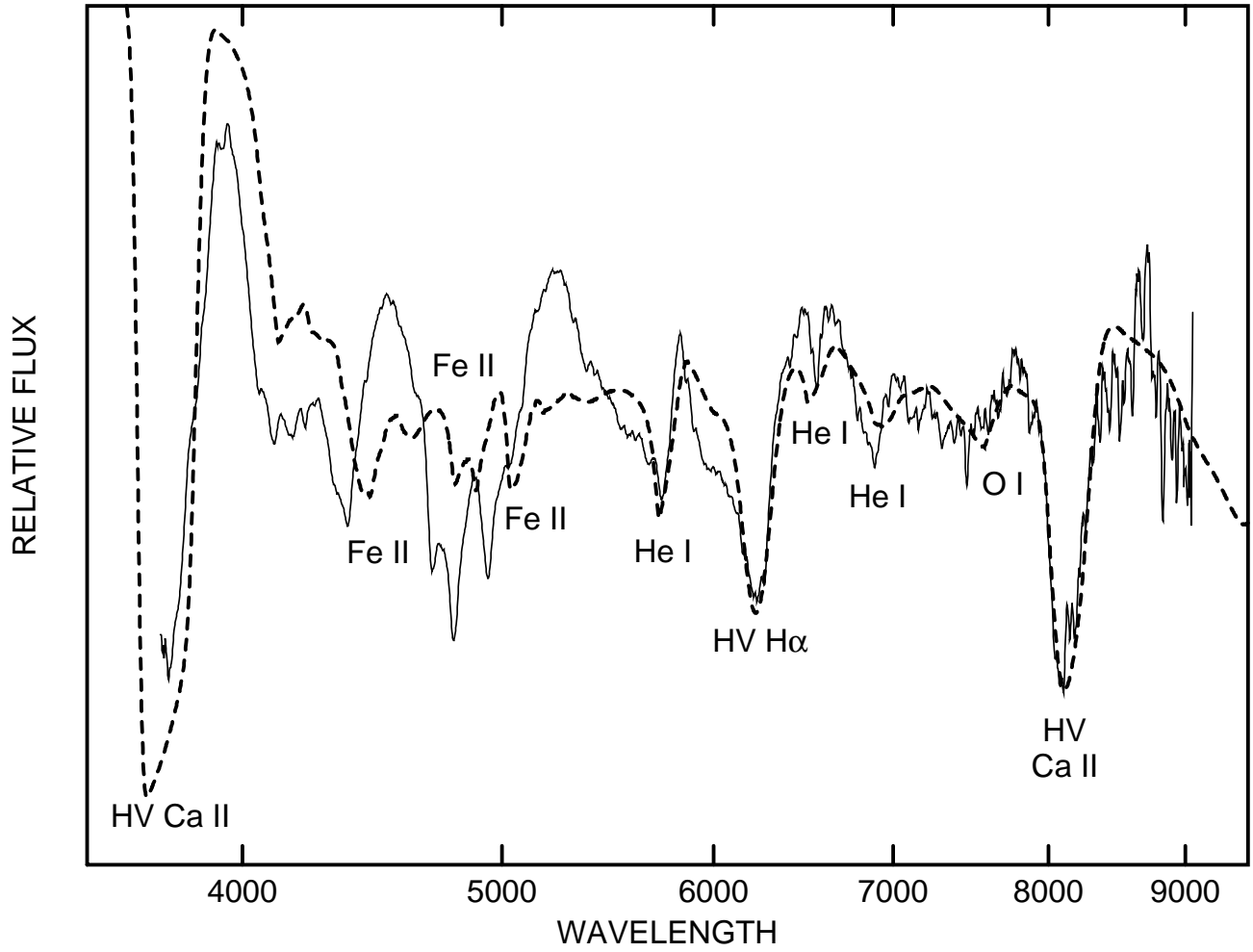


Fig. 4.— Like Figure 3 except that HV Fe II lines have been removed.

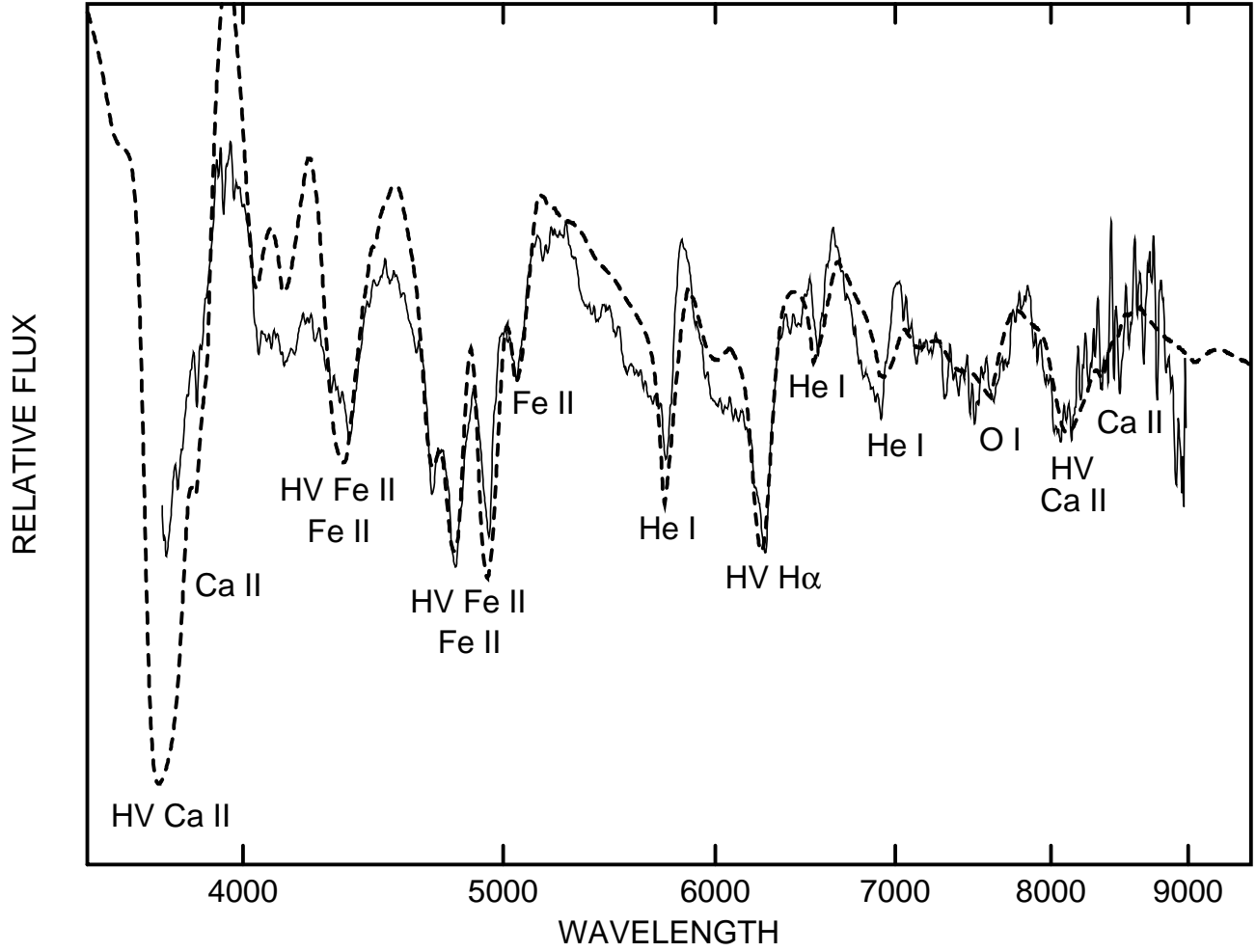


Fig. 5.— The day -27 spectrum of SN 2005bf (*solid line*) is compared with a synthetic spectrum (*dashed line*).

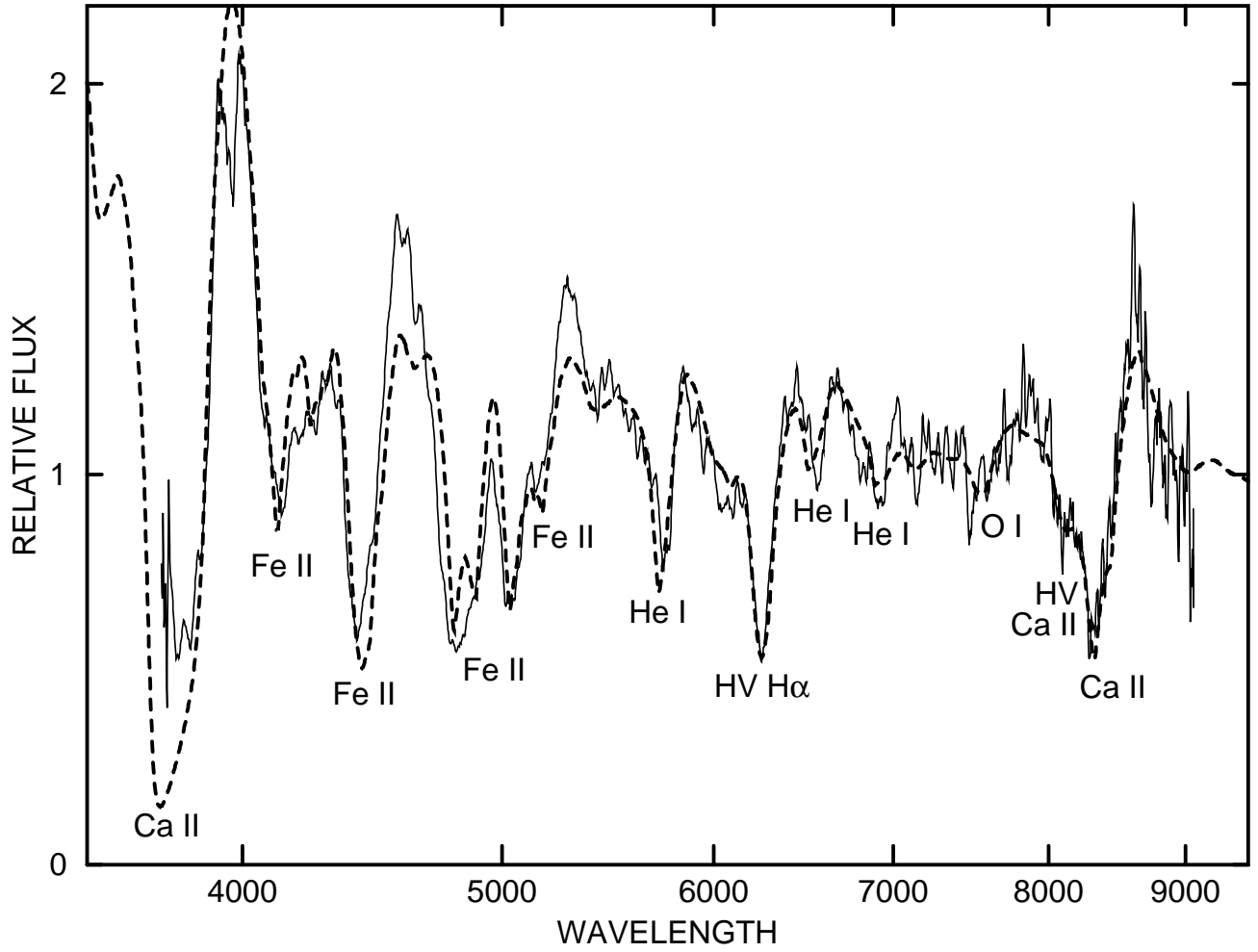


Fig. 6.— The day -20 spectrum of SN 2005bf (*solid line*) is compared with a synthetic spectrum (*dashed line*).

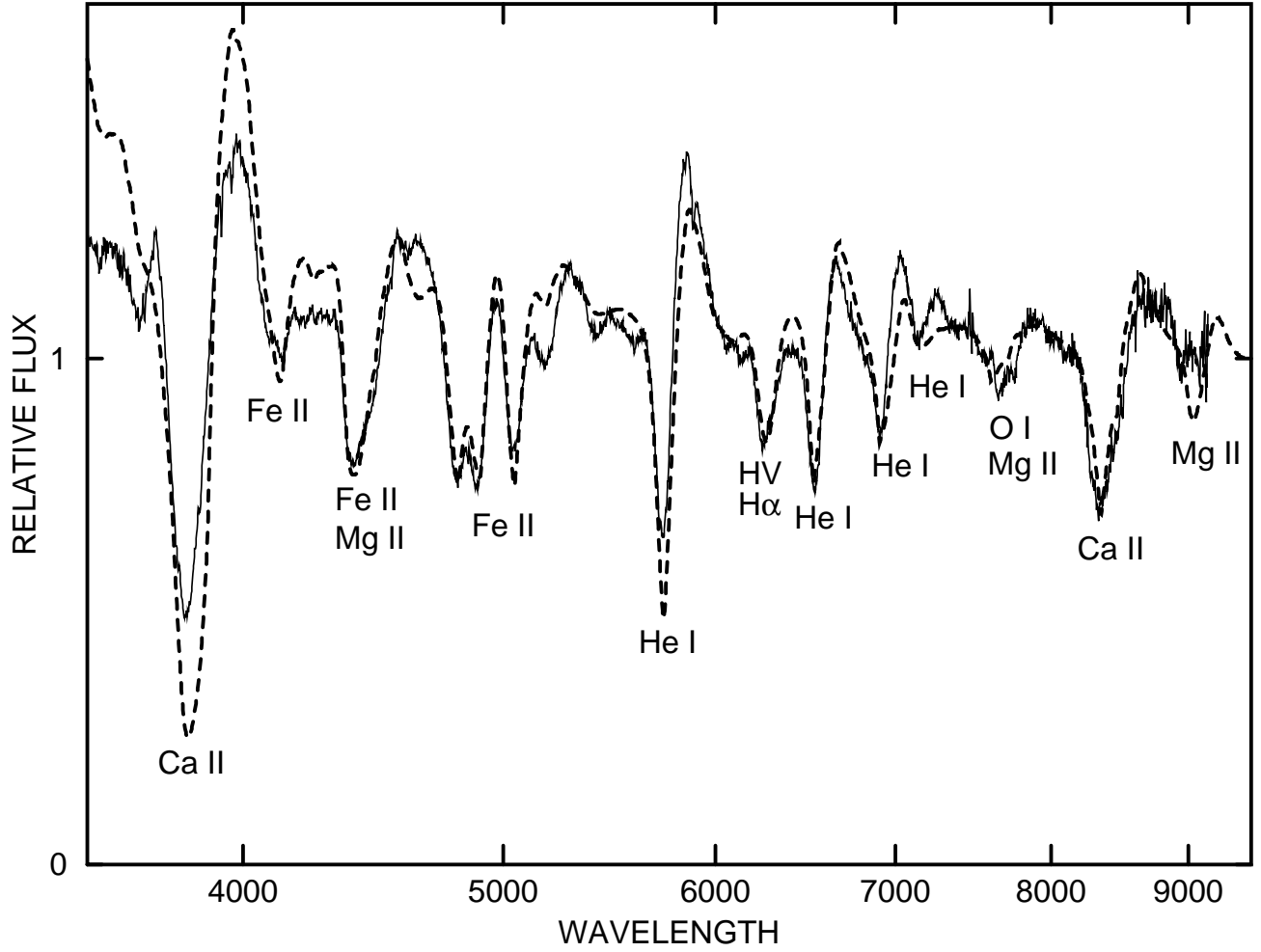


Fig. 7.— The day +2 spectrum of SN 2005bf (*solid line*) is compared with a synthetic spectrum (*dashed line*).

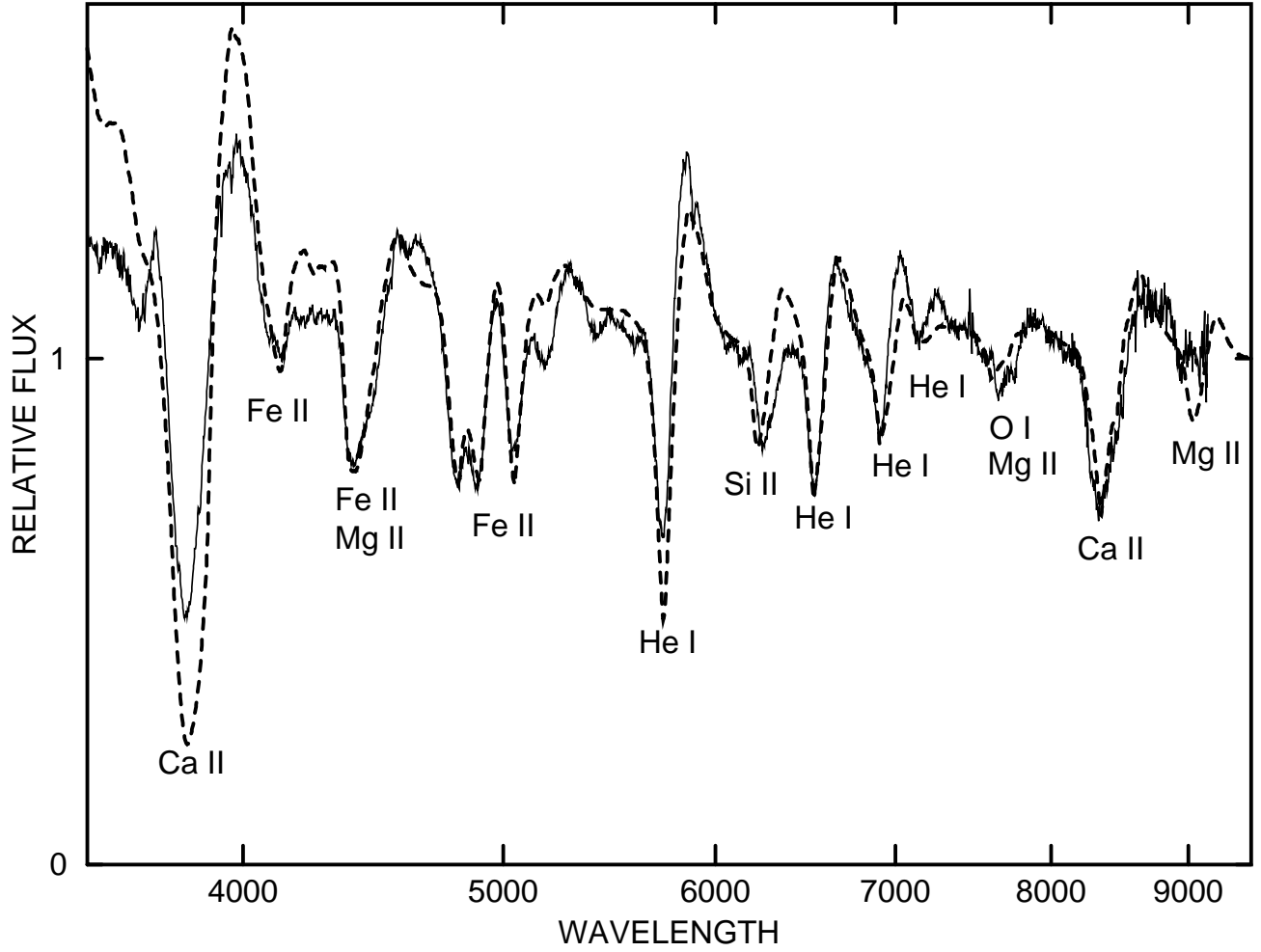


Fig. 8.— Like Figure 5 but with HV hydrogen replaced by PV Si II.

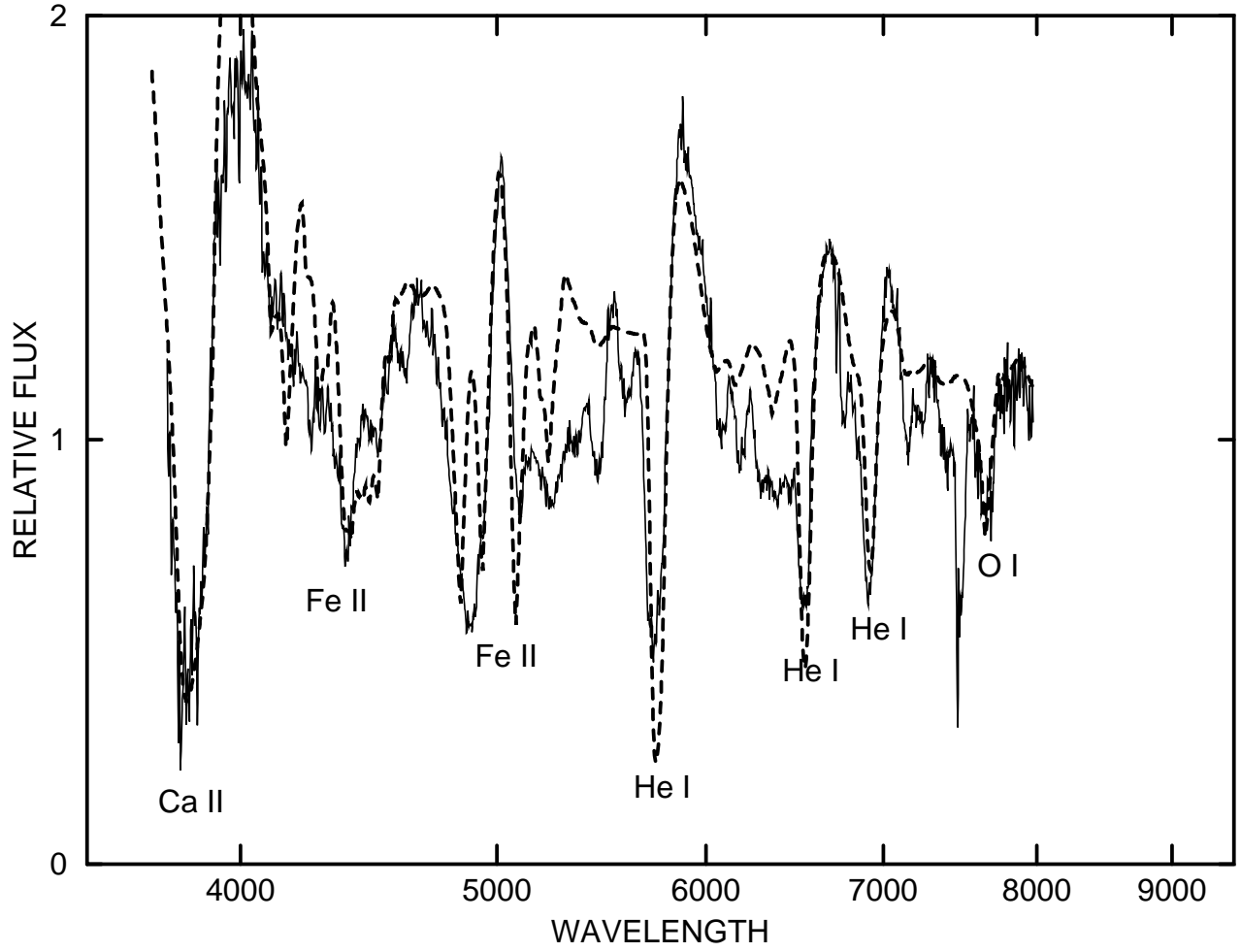


Fig. 9.— The day +21 spectrum of SN 2005bf (*solid line*) is compared with a synthetic spectrum (*dashed line*).

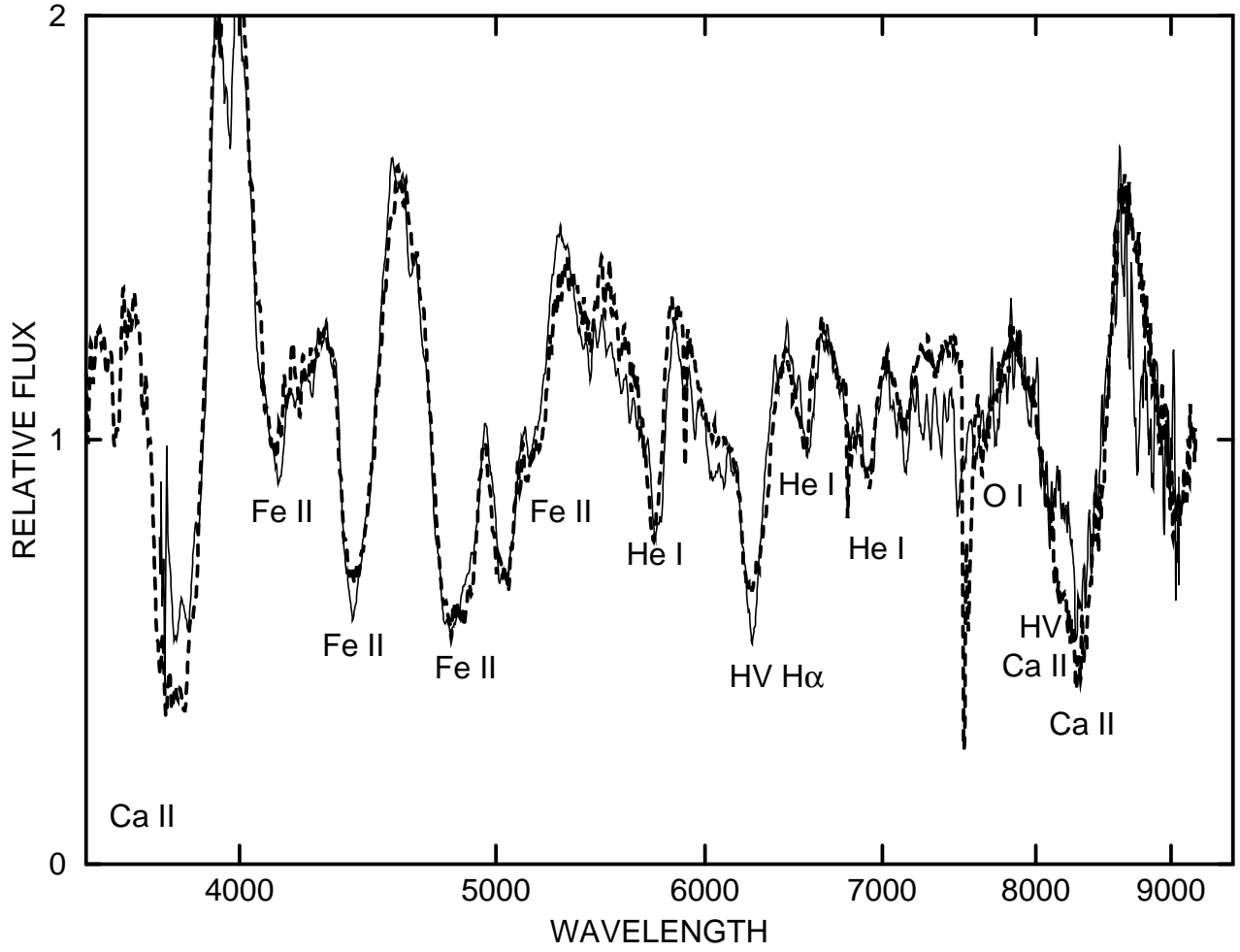


Fig. 10.— A day +5 spectrum of SN 1999ex (*dashed line*) is compared with the day -20 spectrum of SN 2005bf (*solid line*).

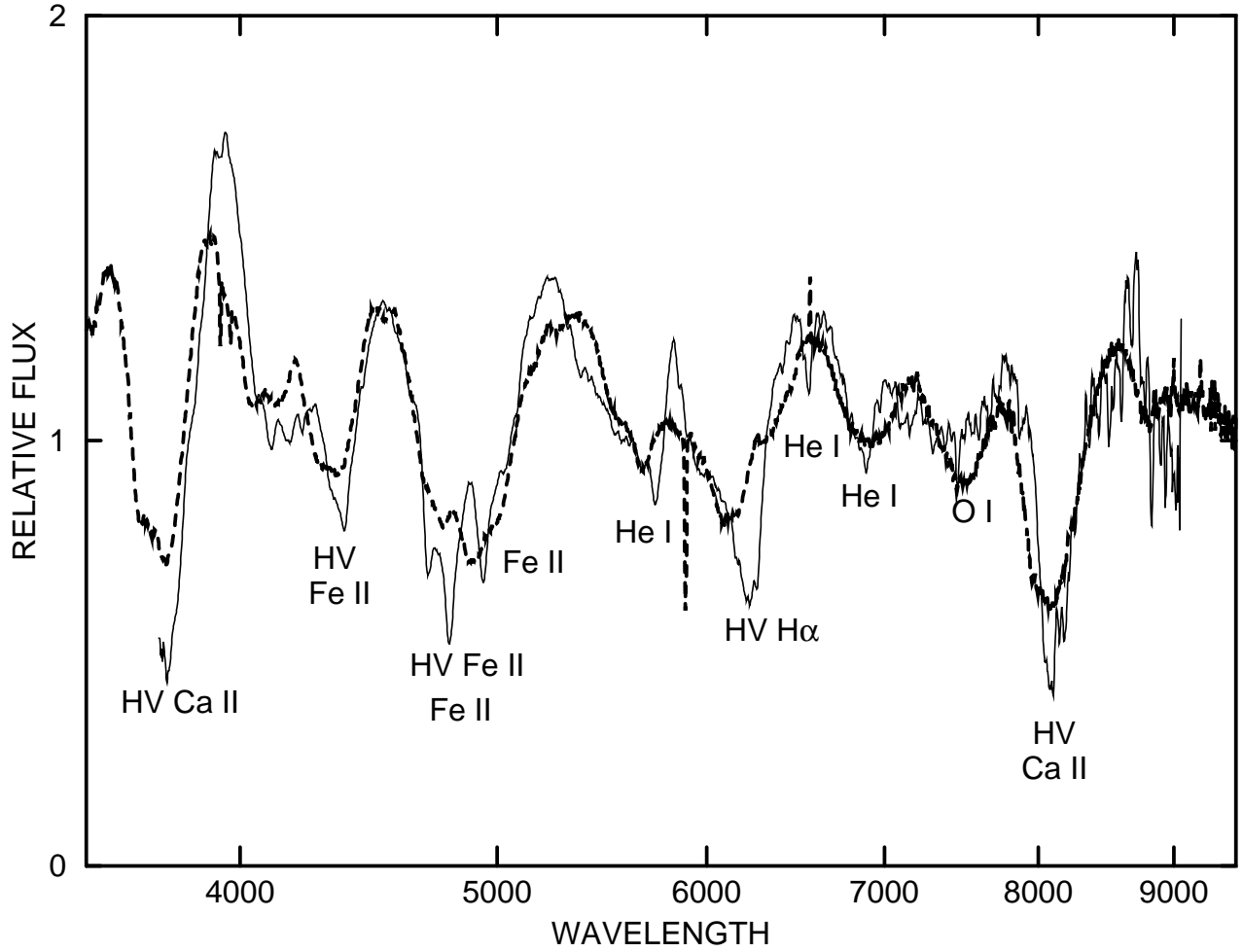


Fig. 11.— A day -4 spectrum of SN 1994I (*dashed line*) is compared with the day -32 spectrum of SN 2005bf (*solid line*).

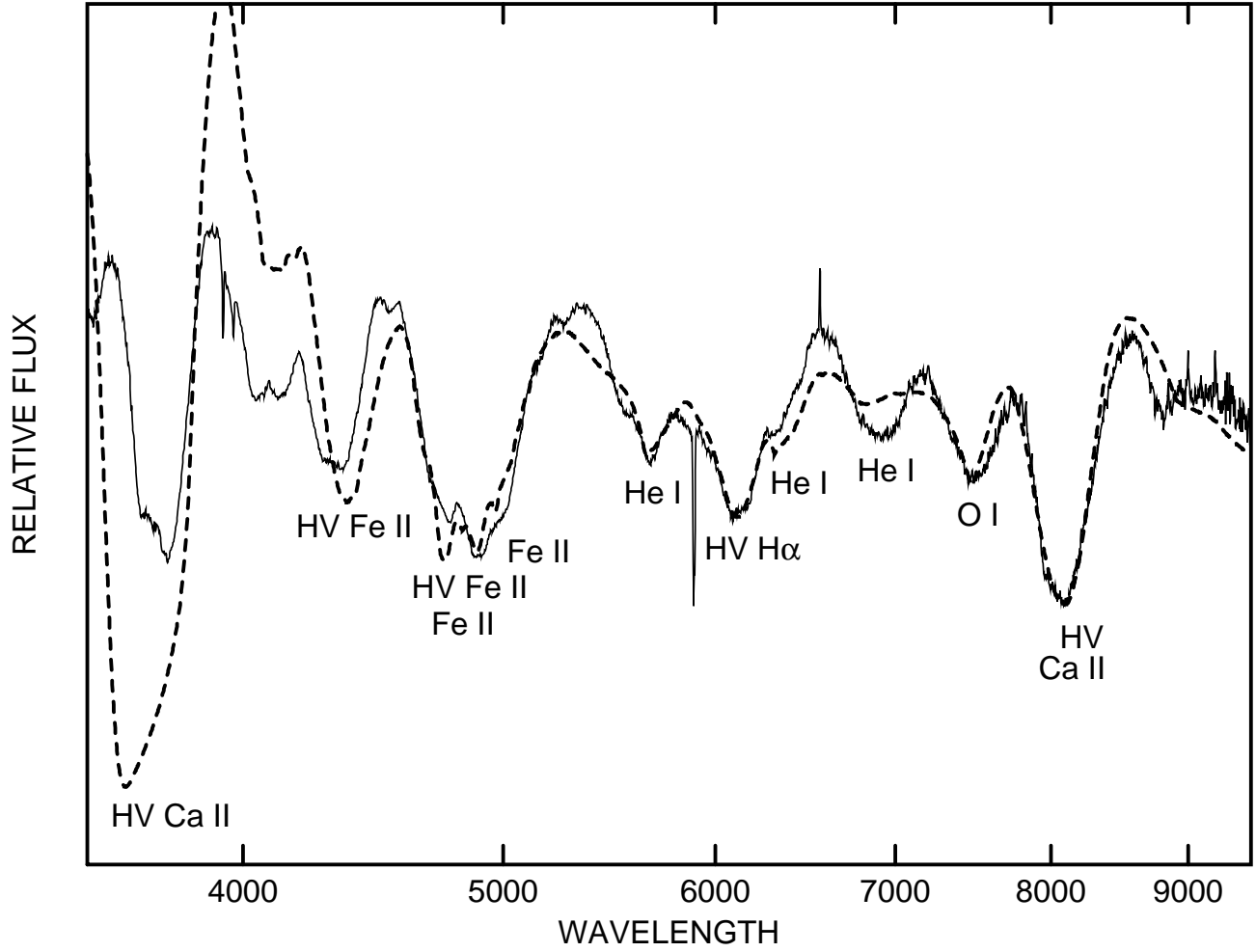


Fig. 12.— The day -4 spectrum of SN 1994I (*solid line*) is compared with a synthetic spectrum (*dashed line*).

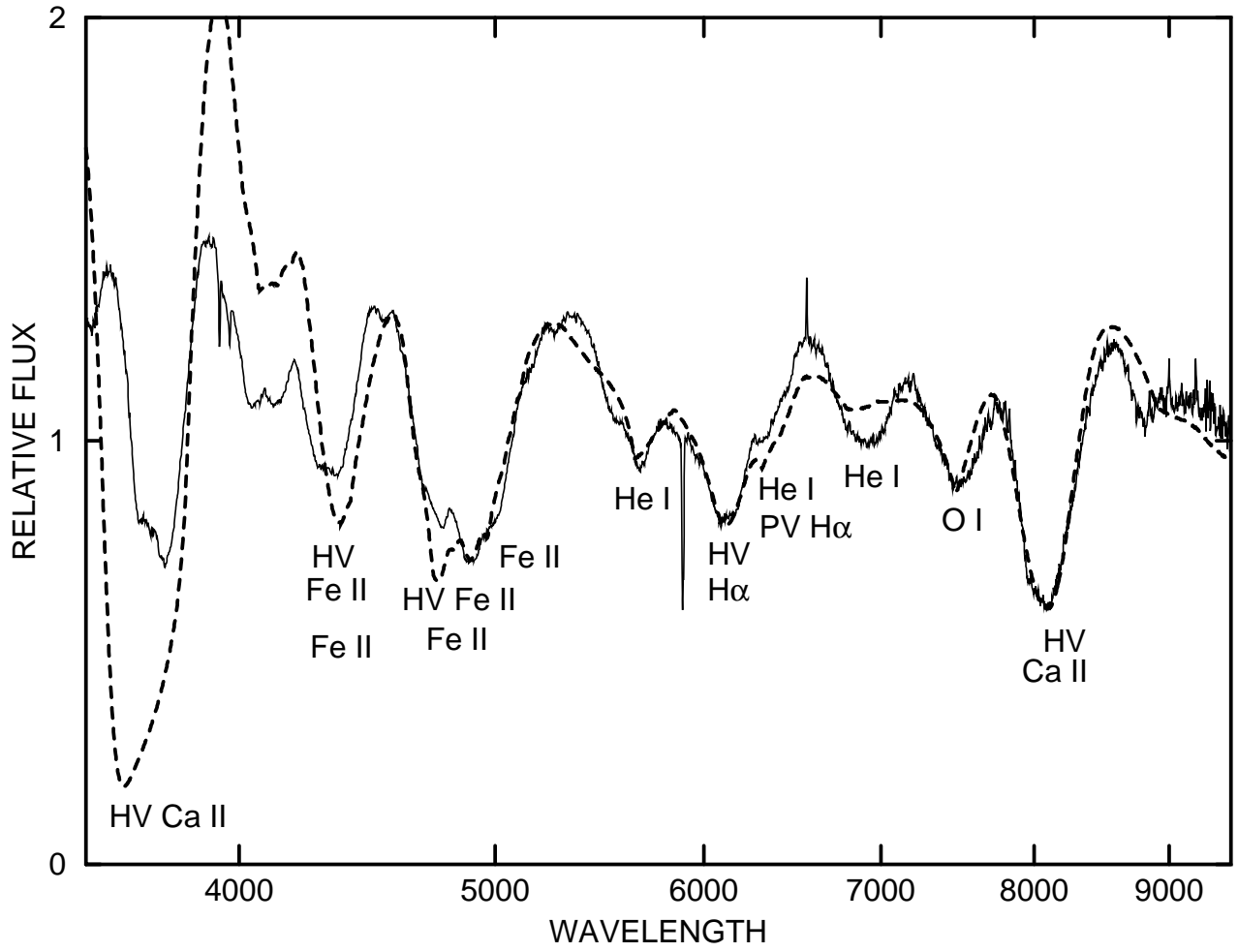


Fig. 13.— Like Figure 12 except that PV H I is included.

Table 1. Fitting Parameters for Synthetic Spectra^a

Parameter	Fig. 2	Fig. 3	Fig. 4	Fig. 5	Fig. 6	Fig. 7	Fig. 12	Fig. 13
v_{phot}	8000	7000	8000	7000	7000	5000	12,000	12,000
$\tau_p(\text{PV H I})$	0	0	0	0	0	0	0	0.6
$n(\text{PV H I})$	8
$\tau_g(\text{HV H I})$	0.7	0.6	0.8	0.25	0	0	0.25	0.25
$v_g(\text{HV H I})$	17,000	16,000	16,000	15,000	23,000	23,000
$\sigma_g(\text{HV H I})$	3000	2000	2000	2000	4000	4000
$\tau_p(\text{PV He I})$	0.8	1.2	1.6	4	4	0	0.3	0.3
$n(\text{PV He I})$	8	8	8	8	8	...	8	8
$\tau_g(\text{PV He I})$	0	0	0	0	0	2.5	0	0
$v_g(\text{PV He I})$	7000
$\sigma_g(\text{PV He I})$	1000
$\tau_p(\text{PV O I})$	0.1	0.12	0.1	0.2	0.2	1	0.3	0.3
$n(\text{PV O I})$	2	2	2	8	8	8	4	4
$\tau_p(\text{PV Mg II})$	0	0	0	0.5	0.5	2	0	0
$n(\text{PV Mg II})$	8	8	8
$\tau_p(\text{PV Si II})$	0	0	0	0	1	0	0	0
$n(\text{PV Si II})$	8
$\tau_p(\text{PV Ca II})$	0	12	150	40	40	40	0	0
$n(\text{PV Ca II})$...	8	8	6	6	4
$\tau_g(\text{HV Ca II})$	25	4	4.5	0	0	0	12	12
$v_g(\text{HV Ca II})$	17,000	17,000	17,000	19,000	19,000
$\sigma_g(\text{HV Ca II})$	2500	2500	2000	6000	6000
$\tau_p(\text{PV Fe II})$	1.5	1	10	0	0	10	2	2
$n(\text{PV Fe II})$	8	8	8	8	8	8
$\tau_g(\text{PV Fe II})$	0	0	0	0.8	0.8	0	0	0
$v_g(\text{PV Fe II})$	8000	8000
$\sigma_g(\text{PV Fe II})$	2000	2000
$\tau_g(\text{HV Fe II})$	1	0.9	0	0	0	0	0.5	0.5
$v_g(\text{HV Fe II})$	15,000	15,000	18,000	18,000
$\sigma_g(\text{HV Fe II})$	2000	2000	2000	2000

^aThe units of v_{phot} , v_g , and σ_g are km s^{-1} .